

Volume XXVI (Issue 4), October-December 2025 1-13

ISSN 2594-0732 FI-UNAM Peer-reviewed article

Article information: Received: October 6, 2024, reevaluated: June 30, 2025, accepted: September 22, 2025.

Attribution-NonCommercial-NoDerivatives 4.0 International (CC BY-NC-ND 4.0) license

https://doi.org/10.22201/fi.25940732e.2025.26.4.032



@**(**)

A conductor subdivision-based method for underground power cable impedance estimation

Elizalde-Camino, Fernando

Universidad de Guadalajara

Centro Universitario de Ciencias Exactas e Ingenierías Departamento de matemáticas, Guadalajara, México E-mail: fernando.elizalde@academicos.udg.mx https://orcid.org/0009-0007-5572-4638

Padilla-González, Marcos

Centro nacional de Control de Energía Gerencia de Control Región Occidente Departamento de Análisis E-mail: mrc-em@hotmail.com https://orcid.org/0009-0007-8013-6520

Ruíz-Prieto, José de Jesús

Centro Nacional de Control de Energía Gerencia de Control Región Occidente Departamento de Análisis E-mail: ingenieur.jose@gmail.com https://orcid.org/0009-0005-9561-7015

Morales-Beltrán, Juan Ramón

Universidad de Guadalajara

Centro Universitario de Ciencias Exactas e Ingenierías

Departamento de Ingeniería Mecánica Eléctrica, Guadalajara, México E-mail: juan.morales@academicos.udg.mx

https://orcid.org/0009-0003-0960-4687

Diaz-Santana, Isai

Universidad de Guadalajara

Centro Universitario de Ciencias Exactas e Ingenierías

E-mail: isai.diaz2995@alumnos.udg.mx https://orcid.org/0009-0005-4227-3749

Hernández-Véliz, Gerardo

Universidad de Guadalajara

Centro Universitario de Ciencias Exactas e Ingenierías

Departamento de Electrónica y Computación, Guadalajara, México

E-mail: gerardo.hze@gmail.com

https://orcid.org/0000-0002-6059-4838

https://orcid.org/0009-0009-1221-8991

Ibarra-Torres, Juan Carlos

Universidad de Guadalaiara

Centro Universitario de Ciencias Exactas e Ingenierías

Departamento de Física, Guadalajara, México E-mail: juan.itorres@academicos.udg.mx

Uribe-Campos, Felipe Alejandro (Corresponding author)

Universidad de Guadalajara

Centro Universitario de Ciencias Exactas e Ingenierías

Departamento de Mecánica Eléctrica E-mail: Felipe.uribe@academicos.udg.mx https://orcid.org/0000-0002-3360-8755

Abstract

This article presents a new version of the subconductor partitioning method for the parametric estimation of the frequency-dependent series impedance of underground cables with concentric and segmental geometry. The main feature of this new proposal is the reduction of the scale factor and the correction of the shape of the subconductors used, with an error control criterion. Thanks to these two techniques, the processing time and computational effort required are significantly reduced, which in previous years probably made this method practically obsolete. This work provides the practical engineer with a new numerical-analytical tool for estimating the frequency-dependent series impedance parameter of power cables, in addition to methods based on electromagnetic theory, such as the finite element method, which is often difficult to implement numerically and requires a certain level of experience when using professional software to adjust the solution obtained to the different types of conductive and dielectric materials that make up the electrical cable under study. The results are validated using the analytical solution for concentric or coaxial cables, based on Schelkunoff's transmission line theory. For cables with arbitrary physical symmetry, validation is performed by applying the finite element method with a change in layer boundary properties at the boundaries for the analysis of the segmented underground elec-

Keywords: Computational electromagnetics, transmission line, conductor subdivision method, finite element method.

Introduction

New power cable technologies require continuous innovation in design techniques to meet the challenges of modern renewable energy projects. More and more wind farms are being constructed offshore each day to support the electrical demand of power systems, transmitting energy via submarine cable links that connect countries' mainland's through high-voltage direct current (HVDC) (Wood *et al.*, 2012; Urquhart & Thomson, 2015; Sutton, 2017; Apostolov & Raymond, 2024; Otani, 2024; Raymond & Komljenovic, 2024; Casey *et al.*, 2023; Modi *et al.*, 2024; Badrzadeh *et al.*, 2024; Bahrani *et al.*, 2024).

Thus, professional software and simulation tools must continuously update to expand the scope of analysis and its reliability limits of submarine and underground cables to include new trends in power and communication application case studies (Ametani, 2015b; Scott-Meyer, 1982; Dommel, 1986; Noda *et al.*, 2008; Ametani, 2015a; Gole, 2004; Dommel, 1972; Ametani, 1980; Ametani *et al.*, 2015; Ametani, 1994).

Some new cable technologies are based on segmental or umbilical cable geometries. These combine power cables with optical fiber cables for communications, ground conductors, and pilot cables for highway bridges in the same trench pipe. They also have many other applications for connecting offshore substation platforms. Unfortunately, there is no widely accepted exact theory or methodology implemented in EMTP-type software that can calculate the electrical parameters of series-impedances (*Z*) and shunt-admittances (*Y*) components for this type of cable geometry (Ametani, 2015b; Scott-Meyer, 1982; Dommel, 1986; Noda *et al.*, 2008; Ametani, 2015a; Gole, 2004; Dommel, 1972; Ametani, 1980; Ametani *et al.*, 2015; Ametani, 1994).

Most commonly used electromagnetic transient and harmonic professional classical software and other simulation tools are limited to analyzing concentric power cables with regular geometries (Schellkunoff, 1934). Consequently, available cable models are only specified for predefined types of configurations with limited conductor/dielectric parameter *ZY* datasets.

Considering these limitations, some numerical subconductor division or partition methods for analyzing power cables with arbitrary cross-sections have emerged (e.g., conductor subdivision methods and partial subconductor equivalent circuits). These methods can complement the use of advanced numerical electromagnetic methods, such as the finite element method (FEM) (De Arizon & Dommel, 1987; Comellini *et al.*, 1973; Lucas & Talukdar, 1978; Graneau, 1979; Rivas & Marti, 2002; Padilla, 2017; Ruiz, 2017; Miki & Noda, 2008; Schmidt *et al.*, 2012; Uribe & Flores, 2018; Cywiński & Chwastek, 2019; Yin & Dommel, 1989; COMSOL; Schött & Walczak, 2021; Guan *et al.*, 2016; Rangelov & Georgiev, 2019).

However, the problem with subconductor partition equivalent methods is the spatial discretization of the cable cross-section image (i.e., the resolution as a function of the skin-effect depth thickness) and the necessary refinement of the subconductor partition, which is a type of optimization process. This results in a substantial increase in computational burden and can make the process very time-consuming (Comellini *et al.*, 1973; Lucas & Talukdar, 1978; Graneau, 1979; Rivas & Marti, 2002; Padilla, 2017; Ruiz, 2017; Miki & Noda, 2008; Schmidt *et al.*, 2012; Uribe & Flores, 2018; Cywiński & Chwastek, 2019; Yin & Dommel, 1989; COMSOL; Schött & Walczak, 2021; Guan *et al.*, 2016; Rangelov & Georgiev, 2019; Zhang *et al.*, 2011).

Because of this drawback, numerical methods based on conductor subdivision are rarely studied or used to estimate *ZY* models of electrical parameters for electromagnetic transient studies or harmonic induction problem analyses.

Thus, this paper proposes a novel scaling technique and a cable shape error compensation technique to increase the numerical efficiency of computing a large electrical parameters data matrix. These techniques can accurately estimate power cable parameters of arbitrary cross-sections and drastically reduce the computational burden and running time as the number of required sub-conductors increases (De Arizon & Dommel, 1987; Padilla, 2017; Ruiz, 2017). The proposal builds on classic work reported in De Arizon and Dommel (1987), Comellini et al. (1973), Lucas & Talukdar (1978), Graneau (1979), Rivas & Marti (2002); and Padilla (2017). It applies a scaled-down spatial sampling dimension of the original cable cross-section, which uses fewer sub-conductors than the original model, without affecting the accuracy of the cable's ZY electrical parameters. It also compensates for cable shape errors when using square or circular sub-conductors (Padilla, 2017; Ruiz, 2017). This process is developed within predetermined accuracy tolerance ranges with a controlled numerical error criterion as a function of resolution. This balances accuracy and simplicity while providing a clear physical interpretation of resistances (R) and inductances (*L*) equivalent electrical circuit components.

CONDUCTOR SUBDIVISION NUMERICAL METHODS

The voltage drop V_n along a transmission line and the circulating currents I_n are related through the well-known first telegrapher equation, which describes a

transmission system propagation model, such as the one shown in Figure 1, formed with two conductors. The resistance and inductance elements (longitudinal effects) of each conductor are represented by R_{nn} and L_{nn} (for n=m) in the main diagonal components of the square matrices in (1). The corresponding mutual inductance components are L_{mn} (for $n \neq m$) on the off-diagonal components of the transmission conductor system matrix (Dommel, 1986; De Arizon & Dommel, 1987; Ruiz, 2017; Cywiński & Chwastek, 2019; Yin & Dommel, 1989).

$$-\frac{d}{dx} \begin{bmatrix} V_1 \\ V_2 \\ \vdots \\ V_n \end{bmatrix} = \begin{bmatrix} R_{11} & R_{12} & \cdots & R_{1,n} \\ R_{21} & R_{22} & \cdots & R_{2,n} \\ \vdots & \vdots & \ddots & \vdots \\ R_{m,1} & R_{m,2} & \cdots & R_{m,n} \end{bmatrix} \begin{bmatrix} I_1 \\ I_2 \\ \vdots \\ I_n \end{bmatrix}$$

$$+j\omega egin{bmatrix} L_{11} & L_{12} & \cdots & L_{1,n} \ L_{21} & L_{22} & \cdots & L_{2,n} \ dots & dots & \ddots & dots \ L_{m,1} & L_{m,2} & \cdots & L_{m,n} \end{bmatrix} egin{bmatrix} I_1 \ I_2 \ dots \ I_n \end{bmatrix}$$

for
$$n, m = 1, 2, 3, ..., N_{cond}$$
 (1)

The resistance and inductance parameters in (1) are defined in per unit length (p.u.l.). It is worth mentioning that the R_{m} and L_{m} elements on the main diagonal of (1) are related to the self-impedance components illustrated along each of the tubular conductors in Figure 1, which represents the longitudinal effects of the transmission system. In contrast, the elements outside the main diagonal of the inductance matrix formulation are related to magnetic coupling effects between the conductors of the system in the presence of the ground-return plane (Noda *et al.*, 2008; Ametani, 2015a; Gole, 2004; Dommel, 1972; Ametani, 1980; Ametani *et al.*, 2015; Ametani, 1994).

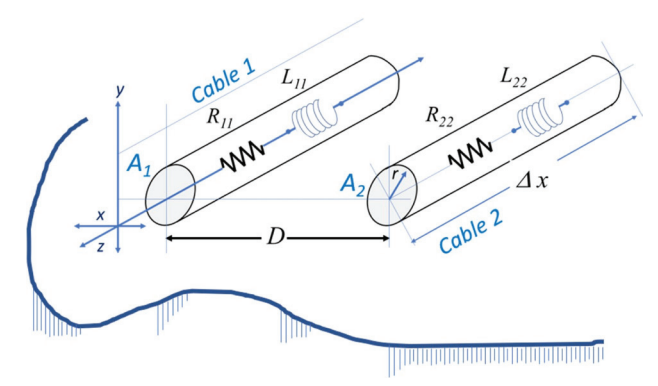


Figure 1. Illustrative description of the First Telegrapher equation according to (1) with longitudinal effects R and L.

THE SCALING REDUCTION TECHNIQUE

According to the conductor subdivision paradigm, the resistance and inductance matrices in (1) increase significantly with the number of subconductors used to partition the original model. This leads to two problems: an increased computational burden and an inability to revert to the original model.

This paper proposes using a downscaling factor on the original cross-section cable model as an image transform (but only for magnitude), which proportionally reduces the dimensions of the cable cross-section geometry. This effectively reduces the number of subconductors, as can be seen in Figure 2 from left to right, from cable 1 to cable 2 with a common ground-return path of reference. Consequently, the computational burden and processing time required to calculate the electrical parameters *R* and *L* for the subconductors of the reduced model are less than those required for the complete original model.

ELECTRICAL PARAMETER DETERMINATION

In classical subconductor partition methods as in De Arizon & Dommel (1987); Rivas & Marti (2022); Comellini *et al.* (1973); Lucas & Talukdar (1978); Graneau (1979), the main idea is to find an equivalent network of subconductors whose electrical properties (*R*, *L*, *G*, and *C*) can describe the real electrical behavior of a power conductor, such as an in the case of aerial line conductor or an underground or submarine cable. On a second step, the subconductor circuit equations system with equal voltages is reduced through a numerical linear algebra method as Kron, Gauss, or Choleski as described in Dommel (1972) into a new set of "bundled" phase conductor equations to find an equivalent to the original electrical conductor system (usually a three phasic system).

However, as the performance of subconductor partition methods (De Arizon & Dommel, 1987; Rivas & Marti, 2022; Comellini *et al.*, 1973; Lucas & Talukdar, 1978; Graneau, 1979) is critically affected by the size, shape, the disposition of the subconductors and by the accuracy of the formulas employed to determine the *R* and *L* parameters, there are some assumptions that must be considered to avoid affecting the results, such as: the cross-section of a homogenous conductor can be subdivided into a number of subconductors (filaments) of equal cross-sectional area (as illustratively shown in Figure 2), the current flows longitudinally in the subconductors, the current density in the conductor is uniform and small enough to each of the partitioned subconductors, the magnetic permeability of a subcon-

ductor is constant throughout the whole cycle of alternating current, but may be different from that of any other subconductor, the conductivity of each subconductor is constant and all the subconductors are in parallel disposition.

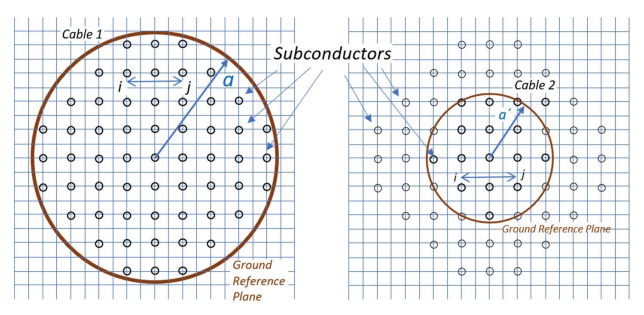


Figure 2. Downscaling factor application to a cable cross-section image from the left-hand side to the right-hand side.

The proposed scaling technique essentially represents a proportional reduction in the cross-section of the conductor as a downscaling factor applied to the exact analytical formulas described in (Schellkunoff, 1934), which take into account the skin effect and proximity effects based on the following:

$$A'_{i} = A_{i} S_{f} \tag{2}$$

where A_i is the original cross-section conductor or cable (as shown in Figure 1), S_f is the downscaling factor (determined empirically), and A'_i is the reduced cross-section of the subconductor.

Thus, the variable change (2) should not significantly affect the behavior of the R and L longitudinal parameters (depicted along each conductor in Figure 1) in the new equivalent electrical circuit concerning the magnitude of the original impedance loop circuit.

Consider now the power cable or conductor shown in Figure 3, which has been taken from (Padilla, 2017; Ruiz, 2017). As shown on the right-hand side of this figure, a scaling factor of 1:2 is applied to this concentric cable. Thus, the computation of *R* and *L* for each subconductor "i" applying the corresponding scaling factor is related to the analytical formulas described in Schellkunoff (1934) with the following:

$$R_i = \frac{\rho_i}{A_i} \propto \frac{\rho_i}{A'_i} \tag{3}$$

Where ρ_i is the resistivity of the metallic conductor "i" and R_i is the metallic conductor resistivity of subconductor "i" under study.

On the other hand, for the calculation of the self and mutual-inductance components of the subconductors

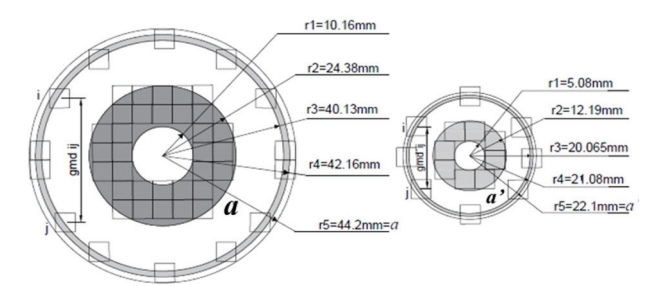


Figure 3. Illustrative coaxial cable model configuration: scaled prototype cable of 2:1 applied in the right-hand side image.

partition in De Arizon & Dommel (1987); Rivas & Marti (2022); Padilla (2017); Ruiz (2017), the method of geometric mean distances (*gmd*) is used to take advantage of the parallel filamental subconductors' position based on the following fundamental expression:

$$\operatorname{In}(gmd_{ik}) = \frac{1}{A_i A_k} \int_{A_k} \int_{A_k} \ln(\tau) dA_i dA_k \tag{4}$$

Where A_i and A_k are the cross-sections of each subconductor, and τ is the distance between subconductors. Thus, the solution of the integral in (4) for square subconductors for the self-*gmd* component:

$$gmd_i = 0.44705 \ \ell$$

Where ℓ is the length of a square shape subconductor, which can be visualized on the right-hand side of Figure 4. For the mutual neighboring (adjacent) subconductors touching each other (Rivas & Marti, 2022):

$$gmd_{ik} = 1.00655 d_{ik}$$

Where d_{ik} is the distance between subconductors i and k. Thus, the self and mutual-impedance components can be evaluated with the following relations:

$$L_{ii} = \frac{\mu_0}{2\pi} \ln \left(\frac{a}{gmd_i} \right) \approx \frac{\mu_0}{2\pi} \ln \left(\frac{a'}{gmd'_i} \right)$$
 (5)

$$L_{ij} = \frac{\mu_0}{2\pi} \ln \left(\frac{a}{gmd_{ii}} \right) \approx \frac{\mu_0}{2\pi} \ln \left(\frac{a'}{gmd'_{ii}} \right)$$
 (6)

Where L_{ii} is the self-inductance (H/m), L_{ij} is the mutual inductance (H/m), μ_0 is the vacuum permeability (H/m), a is the conductor radius of the fictitious ground-return, gmd_i is the geometric-mean distance of each subconductor i and gmd_{ij} is the geometric-mean distance between subconductors i and j. The corresponding downscaling factor quantities are denoted with an apostrophe.

The self and mutual inductance components and the *gmd* for circular subconductors are equivalent to (Schellkunoff, 1934; De Arizon & Dommel, 1987; Rivas & Marti, 2022; Padilla, 2017; Ruiz, 2017) as follows:

$$L_{ii} = \frac{\mu_0}{2\pi} \ln \left(\frac{D^2_{iq}}{D_i D_q} \right) \tag{7}$$

$$L_{ij} = \frac{\mu_0}{2\pi} \ln \left(\frac{D_{iq} D_{jq}}{D_a D_{ii}} \right) \tag{8}$$

Where D_{iq} is the mutual *gmd* between two circles, and for one circle is and $D_i = r_i e^{-\mu i/4}$ and $\mu_i = 1$.

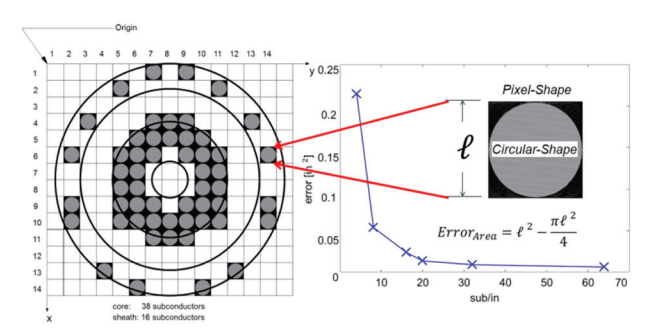


Figure 4. Error compensation between circle and square or pixel subconductor cross-section discretization of the cable conductor.

To include circular subconductors instead of square-shaped ones in the image of Figure 4, two types of errors have to be compensated for. The first one is due to the differences in the area between a circular- and a square-shaped subdivision as a function of the resolution (right-hand side in Figure 4). This can be corrected using the formula shown in the same figure, which represents the error between using a square and a circular shape cross-section.

The second one is due to the use of the approximate formulas (5) and (6) for calculating the *gmd* of square-shaped subconductors (De Arizon & Dommel, 1987; Comellini *et al.*, 1973; Lucas & Talukdar, 1978; Graneau, 1979). This error is corrected using D_{iq} and D_i instead of (5) and (6) when circular-shaped subconductors are applied. According to De Arizon, Dommel (1987); Comellini *et. al.* (1973); Lucas *et. al.* (1978); Graneau (1979), all subconductors inherently introduce this type of error except for the case of two adjacent circular subconductors.

The impact of the shape error compensation technique is shown in the electrical parameter curves in Figure 5, with a spatial resolution of 20 sub/in for the *R* and *L* loop impedances formed between the sheath and core of the power coaxial cable in Figure 3.

As shown in Figure 5a, the resistance (*R*) of the coaxial cable in Figure 3 increases as the effective conducting cross-section decreases according to equation (3) when the frequency of the magnetic flux increases.

This corroborates the idea that the *R* calculation using circular subconductors and the scaling technique is closer to the exact analytical solution of Schellkunoff (1934) than the solution obtained using square-shaped subconductors.

Figure 5b shows the reduction in inductance (*L*) according to the increasing frequency of the alternating magnetic field. The induced current tends to concentrate near the surface of the conductor, which decreases the conductor's effective cross-section for storing magnetic flux links.

Thus, the results obtained indicate that the circular shape with the scaling technique is more accurate for the entire frequency range than the pixel shape.

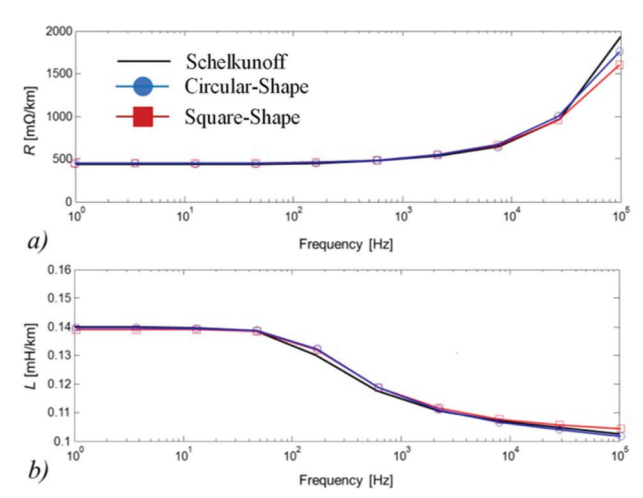


Figure 5. Loop impedance formed between the core and sheath of the cable in Figure 3 as a function of the frequency using a resolution of 20 sub/in. a) Resistance and b) Inductance.

COMPUTATIONAL PERFORMANCE

When using a new algorithm, technique, or methodology, one of the more important features is computer performance, which is measured by complexity, accuracy, and execution time.

For example, in a typical electromagnetic transient simulation using the EMTP-type professional program (Dommel, 1972), if the user decides to use 1,000 samples for the test study, equation system (1) must be solved 1,000 times for an electrical parameter system of size $N_{cond} \times N_{cond}$.

Table 1 shows the accuracy and relative error in calculating the loop resistances and inductances of the cable core-sheath shown in Figure 3 for five different frequencies between 10 Hz and 100 kHz. This was done

using a resolution of 16 sub/in of the analytical solution (Schellkunoff, 1934), the subconductor division method (De Arizon & Dommel, 1987), and the scaling technique developed here.

As an error measure, we decided to use the relative error criterion described as:

$$\varepsilon_{rel}^{\%} = \left| 1 - \frac{f_{approx}}{f_{exact}} \right| \times 100 \tag{9}$$

Where f_{exact} is the improved conductor subdivision numerical method function (here considered as exact) and f_{approx} is the approximated methodology function (approximated results).

As can be seen in Table 1 for a coaxial cable resolution of 16 sub/in, the relative error for resistances *R* is higher at the higher test frequency of 100 kHz, with a value of 5.940 for the implemented version of the conductor subdivision method with respect to the analytical solution. While for the proposed scaling technique, the relative error is slightly less than 5.367.

The higher relative error for the calculated inductances *L* is also higher at 100 kHz for the conductor subdivision method with 1.656, while for the scaling technique, we obtained 0.1949.

To test the computational performance and execution time of the two algorithms under consideration, we chose a resolution rank of 2–20 Sub/in and used 20 samples for the conductor subdivision method in De Arizon & Dommel (1987) and the scaling technique proposed in this work.

Figure 6 shows the results comparing the computer processing elapsed time for each of the two algorithms implemented here. It can be seen from this figure that for resolutions higher than 10 sub/in and above, the proposed scaling technique is approximately one order

of magnitude faster than the conductor subdivision method.

A quantitative analysis of the scaling-reducing technique accuracy behavior as a function of the resolution is shown in Figure 7, testing 4 frequency points, chosen arbitrarily between the range 1 Hz < f < 100 kHz.

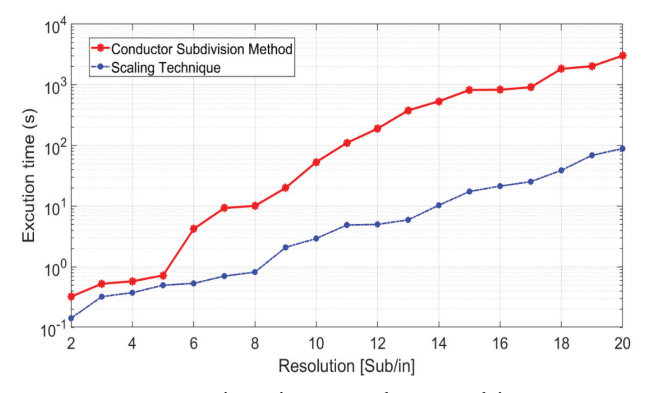


Figure 6. Computer elapsed time as a function of the subconductor resolution.

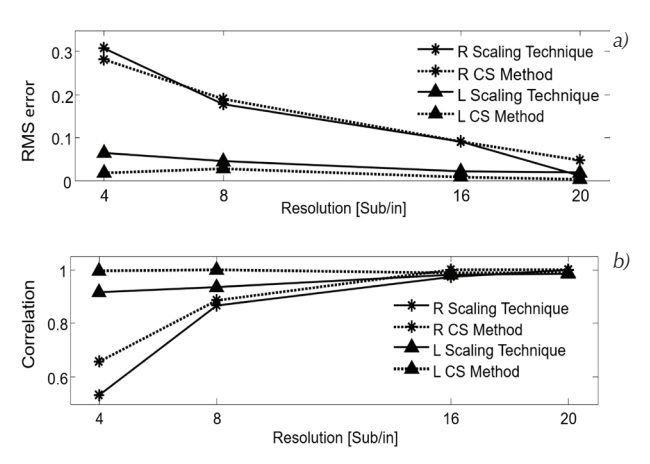


Figure 7. Quantitative analysis of the scaling reducing technique as a function of the resolution: a) RMS Error and b) correlation.

Table 1. Resistances and inductances of the current loop core-sheath of the concentric cable for a resolution of 16 sub/in

Parameter	f (Hz)	Analytical	Conductor subdivision	$\varepsilon^{\%}_{\rm \ rel}$	Scaling technique	$\varepsilon^{\%}_{\rm \ rel}$
	10	416.1	431.4	3.677	417.2	0.264
	100	422.2	436.8	3.458	423.4	0.284
	1k	471.6	489.7	3.838	484.5	1.061
$R (m\Omega/km)$	10k	644.8	652.4	1.178	647.7	0.449
	100k	1835.0	1726.0	5.940	1726.6	5.367
	10	0.1397	0.1392	0.357	0.1393	0.286
	100	0.1350	0.1359	0.666	0.1335	1.111
7 (77/1)	1k	0.1142	0.1154	1.050	0.1156	1.225
L (mH/km)	10k	0.1065	0.1073	0.751	0.1068	0.281
	100k	0.1026	0.1043	1.656	0.1028	0.1949

As can be seen in Figure 7a, the scaling technique has an RMS error slightly higher than the conductor subdivision method (De Arizonv& Dommel, 1987) in the case of 4 Sub/in of resolution. For the other three resolution cases, the RMS error of *R* is lower for the proposed scaling technique.

The correlation factor indicates in Figure 7b the tendency of the results to improve for the proposed scaling technique as the resolution used in the analysis is refined. The results in this work were obtained using a generic personal computer with the following features: Processor Intel ® Core TM i-7-3770 CPU@ 3.40 GHz, RAM: 16.0 GB, 64-bit operating system.

ELECTRICAL SEGMENTAL CABLE ANALYSIS

To analyze the electromagnetic transients of coaxial power cables, the electrical parameters ZY are calculated according to Schellkunoff 's theory using a predetermined number of time-frequency samples in the Laplace domain (Schellkunoff, 1934; Lucas & Talukdar, 1978; Graneau, 1979; COMSOL; Schött & Walczak, 2021; Uribe et al., 2023). When the physical geometry of a three-phase electrical power cable is segmental (see Figure 8; data provided in Table 2), the frequency-dependent electrical parameters can be estimated using the scaling technique (improved partition subconductor numerical method), which is a good alternative due to its combination of scaling reduction and subconductor partition shape error compensation (circular or square shapes). This method offers greater accuracy, reduced computer processing time, and lower algorithmic complexity.

Figure 9 illustrates a 3D graphical layout of the bitmap image arrangement, which was calculated using the MATLAB Image Processing Toolbox (MATLAB, 2017). This layout is for the segmental electrical crosssection power cable calculation shown in Figure 8. These graphical layouts show the positions of the spatial samples in the cross-section of the segmental cable. The pixel information for each of the segmental nuclei and the external sheath can easily be identified in Figure 9, which gives an idea of the number of subconductors that can be used to process the data at a certain resolution. For this numerical representation, the resolution is 46 sub/in using the numerical method of scaling. For illustrative purposes only, the edges of the three conductors are shown in red, orange, and green. The dielectric materials of the internal and external insulators of the segmental cable are represented in blue.

In addition to validating the MATLAB simulation in this paper section of the segmental cable estimated parameters, we used the Finite Element Method (FEM) model implemented in the professional software COM-SOL (COMSOL, 5.3; Padilla, 2017).

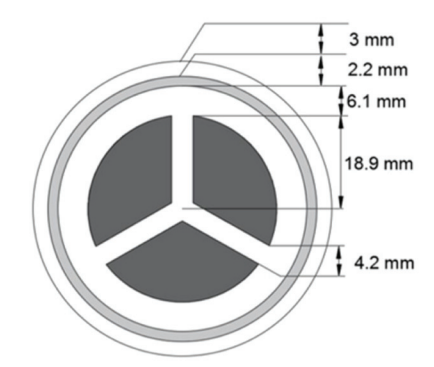


Figure 8. Three-phase power electrical segmental cable.

Table 2. Conductor parameters for power segmental cable in Figure 8.

Conductors	σ (S/mm)	$\mu_{ m r}$	$\mathcal{E}_{\mathbf{r}}$
Cores	58000	1	0
External sheath	1100	1	0
Insulator	0	1	3.3

There are several advantages to using COMSOL for cable parameter numerical estimation problems:

- Irregular, non-concentric geometries: FEM can easily handle non-concentric geometries that traditional analytical methods may struggle with. This makes it suitable for real-world applications where structures are not simple shapes.
- Local refinement: FEM allows for local mesh refinement, meaning you can increase accuracy in areas of interest while maintaining a coarser mesh elsewhere. This adaptability improves parameter estimation without excessive computational costs.
- Material heterogeneity: The method accommodates materials with varying properties, enabling accurate modelling of structures made from multiple materials or those with non-uniform characteristics.
- 4. Nonlinear behaviour: FEM can effectively model nonlinear relationships and behaviours, which are often present in real systems. This flexibility is essential for accurately estimating parameters in systems with complex interactions.
- Integration with optimization: FEM can be seamlessly integrated with optimization algorithms to improve parameter estimation. This integration allows for systematic adjustments and improvements based on iterative feedback from simulations.
- 6. Sensitivity analysis: The method provides an efficient way to perform sensitivity analyses, helping

- us understand how variations in parameters affect the outcome. This understanding is crucial for robust parameter estimation.
- Robustness and stability: FEM is known for its numerical stability, especially when solving partial differential equations. This makes it a reliable choice for parameter estimation tasks.
- 8. Parallel computing: Modern FEM software can leverage parallel computing capabilities to significantly speed up analysis, which is beneficial when dealing with large-scale parameter estimation problems.
- Multiscale analysis: The Finite Element Method (FEM) can be applied to multiscale modelling. This enables the study of phenomena that occur at different scales. It is particularly useful in fields such as materials science and biology.
- Visualization: Results from FEM can be easily visualized, which aids in interpreting data and identifying how parameter changes affect system behaviour (COMSOL).

These benefits make the finite element method (FEM) a valuable numerical tool for addressing the complexities associated with non-arbitrary cable parameter validation in various study cases.

However, using COMSOL Professional software is neither simple nor quick to learn. In other words, it is possible to handle generic routines in the first session, but when it comes to modelling more serious or complex problems, a great deal of experience and a long period of technical learning are required.

The mesh depicted in Figure 10 was created using the boundary layer meshing technique, a professional routine available from COMSOL which automatically comprises 285516 elements and 147023 mesh vertices at a test frequency of 640 kHz, and was applied to each core conductor, considering the material's conductivity and the complex skin-effect layer-thickness (δ) approximated as Dommel (1986); Noda *et al.* (2008); Ametani (2015b):

$$\delta \approx 503 \cdot \sqrt{\frac{\rho}{f}} \tag{10}$$

Where Ω ·m is the conductor material resistivity and f (Hz) is the oscillating system frequency.

The magnetic field intensity distribution of each conductor phase of the cable was obtained by energizing the three cores simultaneously with a 1 V p. u. Potential. In this case, the return current is negative, and its magnitude equals the sum of the three core circulating currents.

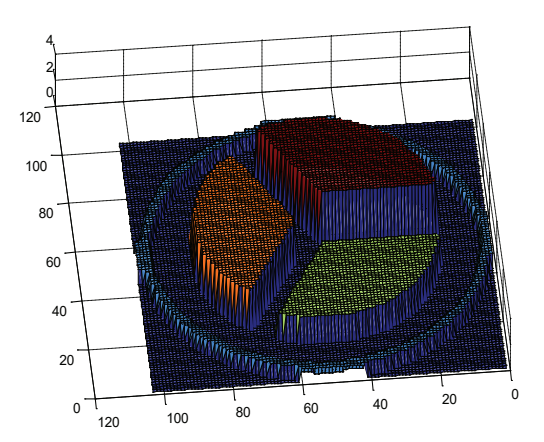


Figure 9. 3D graphical layout view of the bitmap image of the segmental cable.

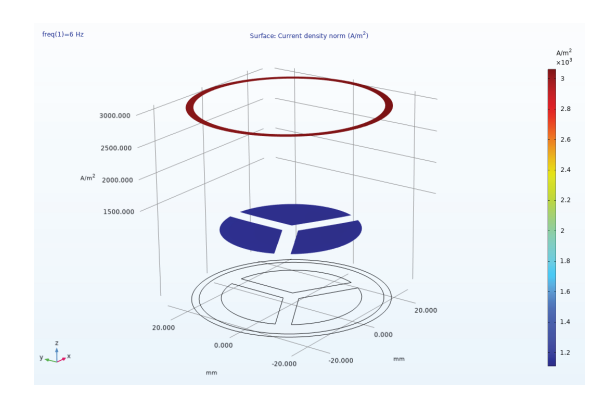


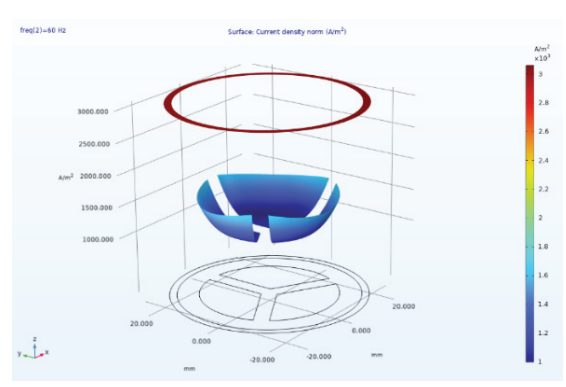
Figure 10. Automatically mesh generated with FEM and the boundary layer meshing routine available in COMSOL with 285516 triangular elements for the electrical segmental cable in Figure 8.

Figure 11 shows the uniform distribution of current density in the core and sheath of the segmental cable. At a very low frequency, such as 6 Hz, the current flows homogeneously through the core of the cable, and the skin effect is not visible. The same behaviour is observed in the sheath. At an operating power frequency of 60 Hz, a slight concentration of current becomes noticeable at the periphery of the conductors. The onset of the skin effect is subtle, as the current density is slightly higher at the outer edge. At 6 kHz, the proximity and skin effects are more evident. The current is concentrated in a thin region of the conductor because the interior of the conductor does not carry current due to the skin effect. A pattern is also observed in the current density: It is zero in the centre of the cable due to the proximity effect caused by the 120° symmetrical distribution of the three conductors within the cable. These two effects contribute to greater losses due to increased resistance and affect temperature dissipation and the cable's inductive effect.

a)

b)





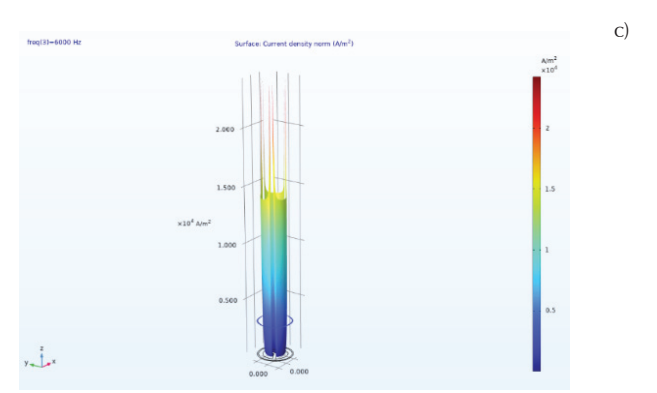


Figure 11. Surface current density distribution in a segmental three-phase shielded cable: comparison of frequency effects and skin effect at: a) 6 Hz, b) 60 Hz, and c) 6 kHz.

Figure 12 shows the distribution of magnetic flux density at a frequency of 60 kHz as simulated using COM-SOL. As can be seen in the figure, the shape of the core conductors and their 120-degree arrangement limit the magnetic flux density to the outer edges of the three wires, causing it to decrease toward the shielding. This behaviour is produced by the combination of the skin effect and the proximity of the core conductors.

Figure 13 shows the loop resistances and inductances for the self and mutual components between the cores and the sheath of the segmental cable, applying the proposed scaling technique and the shape error compensation between the square and the circular sha-

pe subconductor formulas validated with FEM using COMSOL (Padilla, 2017).

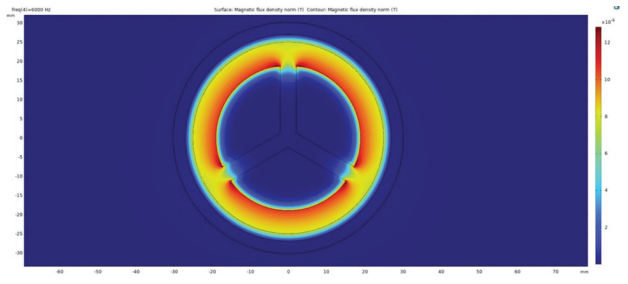


Figure 12. Magnetic flux density distribution at 60 kHz obtained with FEM using COMSOL (Yin & Dommel, 1989; Modi *et al.*, 2024).

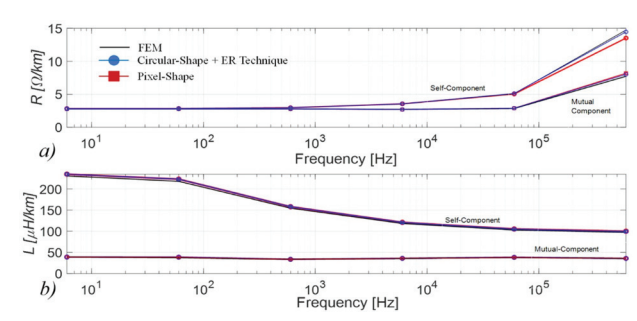


Figure 13. Loop impedance validation formed between the core and sheath of the segmental cable shown in Figure 8 as a function of the frequency. a) Resistances and b) Inductances.

The increasing magnitude behaviour of the loop-resistance curves along frequency in Figure 13a is due to the effective area reduction of the current density according to the skin and proximity effects, while the decreasing magnitude of inductance with frequency in Figure 13b is due to the reduction in magnetic flux as the effective area of the conductor decreases (Lucas & Talukdar, 1978; Graneau, 1979; Rivas & Marti, 2002; Padilla, 2017). It can be seen from Figure 13 that the conductor subdivision method for circular and rectangular (pixel) shapes and the FEM-based results are in good agreement for self and mutual resistances and inductance components.

The corresponding relative errors for the self and mutual-loop impedance components for seven different frequencies arbitrarily chosen are given in Tables 3 and 4, respectively. The relative errors between both sets of curve impedances were calculated with the relative error function in (9).

The computational processing times required for estimating the R and L parameters for each frequency are approximated and shown repeatedly in Tables 2 and 3, for each case of self-impedance or mutual-impedance, respectively, as the COMSOL program solves the integro-differential equations of electromagnetic theory together for each pair of parameter sets.

These processing time records will depend on the type of computer used, the operating system running, and the type of processing, cores, and memory capacity assigned to perform the simulation in COMSOL exclusively.

The COMSOL simulation developed in this study was run on a desktop PC with an AMD64 Family 21 Model 101 processor with one socket and four cores. The simulation utilized 16 GB of available RAM, 5 GB of physical memory, and 5.3 GB of virtual memory.

The total solution time required to estimate the electrical parameters R and L of the segmental cable study in COMSOL, using seven frequency samples shown in Tables 3 and 4 within the range of 6 Hz to 640 kHz, was approximately 1,495 seconds (almost 25 minutes per case). This reflects the model's complexity due to the

fine mesh and the variety of materials used as conductors and dielectrics. Such times are typical when seeking an accurate simulation of frequency-dependent parameters, mutual inductances, or field distribution in multi-conductor configurations.

The results shown in Tables 3 and 4 confirm the accuracy of the method proposed here as a scaling factor with circular or square shape correction with respect to the FEM method using COMSOL as validation. The maximum relative percentage error was obtained in the estimation of the inductive component in the mutual impedance loop with a value of 3.561 %. Since the frequency study range is considered wide, from 6 Hz to 640 kHz, this error value can be considered very low. This error occurs in the power frequency component of the electrical network.

Table 3. Relative errors between the proposed method and fem for the self-loop impedance of the segmental cable for a resolution of 46 sub/in.

Parameter	f (Hz)	FEM	Processing time (s)	Scaling technique	Processing time (s)	${\mathcal E}^{\%}_{{ m rel}}$
	6	0.00284	42	0.002839	46	0.039719
	60	0.00285	67	0.002849	62	0.030065
	600	0.002967	78	0.002968	84	0.042023
D (O/L)	6k	0.003535	105	0.003557	92	0.632206
$R (\Omega/\mathrm{km})$	60k	0.005088	110	0.005053	101	0.690415
	600k	0.014731	129	0.014332	136	2.708455
	640k	0.015226	204	0.014781	174	2.924796
	6	2.31E-07	42	2.35E-07	51	1.910963
	60	2.18E-07	67	2.24E-07	62	2.400467
	600	1.55E-07	78	1.58E-07	84	2.354003
T / TT/I	6k	1.18E-07	105	1.21E-07	92	2.357915
L (μH/km)	60k	1.03E-07	110	1.05E-07	101	2.376004
	600k	9.76E-08	129	1.00E-07	136	2.698865
	640k	9.75E-08	204	1.00E-07	174	2.709231

Table 4. Relative errors between the proposed method and FEM for the Mutual-loop impedance of the segmental cable for a resolution	on
of 46 Sub/in.	

Parameter	f (Hz)	FEM	Processing time (s)	Scaling technique	Processing time (s)	$arepsilon^{\%}_{ m rel}$
	6	0.00278	38	0.002781	52	0.039297
	60	0.00278	76	0.002782	63	0.03573
	600	0.00278	88	0.002783	74	0.001852
- (O.)	6k	0.00270	95	0.002699	82	0.221935
$R\left(\Omega/\mathrm{m}\right)$	60k	0.00284	110	0.002875	94	1.015144
	600k	0.00772	123	0.007758	115	0.446325
	640k	0.00798	217	0.007956	183	0.329252
	6	3.93E-08	38	3.94E-08	52	0.20384
	60	3.77E-08	76	3.90E-08	63	3.561305
	600	3.36E-08	88	3.39E-08	74	0.818055
	6k	3.59E-08	95	3.61E-08	82	0.659637
<i>L</i> (H/m)	60k	3.80E-08	110	3.85E-08	94	1.362527
	600k	3.59E-08	123	3.60E-08	115	0.234113
	640k	3.59E-08	217	3.60E-08	183	0.222434

Although the differences in processing time between the method proposed here and those obtained with COMSOL FEM are not very different, as expected, there is the possibility of reducing them even further in the proposed method by using a different operating system platform, such as Linux (Ubuntu).

CONCLUSIONS

This paper presents the scale factor method with shape correction in circular and square subconductors, which is accurate and relatively fast for estimating the electrical parameters R and L of coaxial and segmental cables for underground electrical power transmission and distribution. For the case study of coaxial cables, the results obtained from the method proposed here were compared with a version of the subconductor partitioning method implemented here (De Arizon & Dommel, 1987), and for the case study of segmental cables, it was validated with the FEM method using the professional simulation program COMSOL. For the coaxial cable estimate, the maximum relative percentage error is less than 6 %, while for the segmental cable, the maximum relative percentage error is less than 4 %. With regard to the processing time for estimating coaxial cable parameters, the scaling factor technique proposed here for resolutions greater than 10 sub/in is at least an order of magnitude faster than the version of the conductor subdivision method implemented here (De Arizon & Dommel, 1987). With regard to the processing time required by COMSOL for parametric estimation, the difference is small, but it is slightly favorable for the technique proposed here. With this, the challenge of improving the numerical implementation of the scaling technique may be an open issue for programmers in operating systems and computationally efficient programming languages.

NOMENCLATURE

ω	angular frequency (in rad/s)
$\mu_{\scriptscriptstyle 0}$	magnetic permeability of vacuum (H/m)
σ	electrical conductivity (S/m)
$\rho_{\scriptscriptstyle n}$	resistivity of a conductor material " n " ($\Omega \cdot m$)
ε_n	dimensionless relative permittivity of a material " n "
D	distance between conductors (m)
p	complex Skin Effect layer thickness $p = 1 / \sqrt{(j\omega\mu_0\sigma)}$
δ	real depth of the Skin Effect layer thickness $\delta \approx 503 \cdot \sqrt{(\rho/f)}$
	- (4.7)
A_i	cross-section of conductor "i"
A_i h	
•	cross-section of conductor "i"
h	cross-section of conductor "i" cable heigth (m)
h S_f	cross-section of conductor "i" cable heigth (m) downscaling factor
h S_f r_n	cross-section of conductor "i" cable heigth (m) downscaling factor underground cable core radius (m)
h S_f r_n l	cross-section of conductor "i" cable heigth (m) downscaling factor underground cable core radius (m) conductor length (m)
h s_f r_n l s	cross-section of conductor "i" cable heigth (m) downscaling factor underground cable core radius (m) conductor length (m) Laplace complex variable
h s_f r_n l s Z	cross-section of conductor "i" cable heigth (m) downscaling factor underground cable core radius (m) conductor length (m) Laplace complex variable series-impedance (p.u.l)

- G conductance (p.u.l)
- C capacitance (p.u.l)
- V voltage (V)I current (A)
- N_{cond} total number of conductors

DECLARACIÓN DE INTERÉS EN COMPETENCIA

Los autores declaran que no tienen intereses financieros en competencia ni relaciones personales conocidas que pudieran haber influido en el trabajo informado en este documento.

Códigos de clasificación: 220203 & 330605

REFERENCES

- Ametani A. (1994). *Cable parameters rule book*. Portland, Oregon: B.P.A. USA.
- Ametani, A. (1980). A general formulation of impedance and admittance of cables. *IEEE Transactions on Power Apparatus and Systems*, PAS-99(3), 902-910. https://doi.org/10.1109/tpas.1980.319718
- Ametani, A. (2015a). Chapter 5 "XTAP", Numerical analysis of power system transients and dynamics. The Institution of Engineering and Technology (IET). Retrieved on https://www.xtap.org/
- Ametani, A. (2015b). Numerical analysis of power system transients and dynamics.
- Ametani, A., Ohno, T., & Nagaoka, N. (2015). *Cable system transients: Theory, modeling and simulation*. John Wiley & Sons.
- Apostolov, A., & Raymond, J. (2024). The electric power systems of the future: Still progress to be made [In my View]. *IEEE Power and Energy Magazine*, 22(3), 112-116. https://doi.org/10.1109/mpe.2024.3366503
- Badrzadeh, B., Cardozo, C., Hishida, M., Shah, S., Huq, I., Modi, N., & Morton, A. (2024). Grid-Forming inverters: Project demonstrations and pilots. *IEEE Power and Energy Magazine*, 22(2), 66-77. https://doi.org/10.1109/mpe.2023.3342766
- Bahrani, B., Ravanji, M. H., Kroposki, B., Ramasubramanian, D., Guillaud, X., Prevost, T., & Cutululis, N. (2024). Grid-Forming Inverter-Based resource research landscape: Understanding the key assets for renewable-rich power systems. *IEEE Power and Energy Magazine*, 22(2), 18-29. https://doi.org/10.1109/mpe.2023.3343338
- Casey, L., Enslin, J. H., Joós, G., Siira, M., Borowy, B., & Sun, C. (2023). Advanced inverter interactions with electric grids. *IEEE Power Electronics Magazine*, 10(2), 20-27. https://doi. org/10.1109/mpel.2023.3271619
- Comellini, E., Invernizzi, A., & Manzoni, G. (1973). A computer program for determining the electrical resistance and reactance of any transmission line. *IEEE Transactions on Power Appara-*

- tus and Systems, PAS-92(1), 308-314. https://doi.org/10.1109/tpas.1973.293628
- COMSOL Multiphysics reference manual, Version 5.3, COMSOL, Inc. Retrieved on www.comsol.com
- Cywiński, A. & Chwastek, K. (2019). Modeling of skin and proximity effects in multi-bundle cable lines. *Progress in Applied Electrical Engineering (PAEE)*, pp. 1-5. https://doi.org/10.1109/PAEE.2019.8788986
- De Arizon, P. & Dommel, H. W. (1987). Computation of cable impedances based on subdivision of conductors. *IEEE Transactions on Power Delivery*, 2(1), 21-27. https://doi.org/10.1109/tpwrd.1987.4308068
- Dommel, H. (1972). User's manual for program: Line constants of overhead lines. Portland: B.P.A, USA.
- Dommel, H. (1986). EMTP Theory Book. Portland, Oregon: B.P.A, USA.
- Gole, A. (2004). *Manitoba HVDC Research Centre. User's Guide on the Use of PSCAD*. Winnipeg, Manitoba, Canada: Winnipeg.
- Graneau, P. (1979). *Underground power transmission*. New York, USA: John Wiley & Sons.
- Guan, H. et al. (2016). Simulation calculation for the total electric field of a three-phase power cable. On 2016 IEEE International Conference on High Voltage Engineering and Application (ICHVE), pp. 1-4. Retrieved on https://doi.org/10.1109/ ICHVE.2016.7800883
- Lucas, R., & Talukdar, S. (1978). Advances in finite element techniques for calculating cable resistances and inductances. *IEEE Transactions on Power Apparatus and Systems*, PAS-97(3), 875-883. https://doi.org/10.1109/tpas.1978.354559
- MATLAB (2017). Natick, Massachusetts. The Mathworks, Inc. 9.3.0.713579 R2017b. Retrieved on www.matlab.com
- Miki, T., & Noda, T. (2008). An improvement of a conductor subdivision method for calculating the series impedance matrix of a transmission line considering the skin and proximity effects. *IEEJ Transactions on Power and Energy*, 128(1), 254-261. Released on J-STAGE January 01, 2008. Online ISSN 1348-8147, Print ISSN 0385-4213, https://doi.org/10.1541/ieejpes.128.254, and https://www.jstage.jst.go.jp/article/ieejpes/128/1/128_1_254/_article/-char/en
- Modi, N., Escudero, M. V., Aramaki, K., Zhou, X., & Partinen, P. (2024). High inverter-based resource integration: The experience of five system operators. *IEEE Power and Energy Magazine*, 22(2), 78-88. https://doi.org/10.1109/mpe.2023.3341794
- Noda, T., Takenaka, K., & Inoue, T. (2008). Numerical integration by the 2-Stage diagonally implicit Runge-Kutta method for electromagnetic transient simulations. *IEEE Transactions on Power Delivery*, 24(1), 390-399. https://doi.org/10.1109/tpwrd. 2008.923397
- Otani, T. (2024). Power grids achieving carbon neutrality with a reduced labor force: Energy management and automation Systems cooperation. *IEEE Power and Energy Magazine*, 22(3), 20-28. https://doi.org/10.1109/mpe.2023.3344557

- Padilla, M. (2017). El método de subdivisión de conductores para cables de potencia sectoriales. (Tesis de maestría en ciencias en ingeniería eléctrica). CUCEI, Universidad de Guadalajara, Jalisco, México.
- Rangelov, Y. & Georgiev, D. (2019). Short-circuit analysis in high-voltage transmission systems with a large share of underground cables. On 11th Electrical Engineering Faculty Conference (BulEF). pp. 1-4. Retrieved on https://doi.org/10.1109/BulEF48056.2019.9030751
- Raymond, J., & Komljenovic, D. (2024). Situational awareness: a road map to generation plant modernization and reliability. *IEEE Power and Energy Magazine*, 22(3), 29-41. https://doi.org/10.1109/mpe.2023.3348430
- Rivas, R., & Marti, J. (2002). Calculation of frequency-dependent parameters of power cables: Matrix partitioning techniques. *IEEE Transactions on Power Delivery*, 17(4), 1085-1092. https://doi.org/10.1109/tpwrd.2002.803827
- Ruiz, J. (2017). Estimación de transitorios en cables de potencia mediante los métodos de subdivisión de conductores y elemento finito. (Tesis de maestría en ciencias en ingeniería eléctrica). CUCEI, Universidad de Guadalajara, Jalisco, México.
- Schelkunoff, S. A. (1934). The electromagnetic theory of coaxial transmission lines and cylindrical shields. *The Bell System Technical Journal*, 13, 532-539
- Schmidt, U., Shirvani, A., & Probst, R. (2012), An improved algorithm for determination of cable parameters based on frequency-dependent conductor segmentation. On IEEE PES Transmission and Distribution Conference and Exposition, pp. 1-7. Retrieved on https://doi.org/10.1109/tdc.2012.6281601
- Schött-Szymczak, A. & Walczak, K. (2021). Impact of cable configuration on the voltage induced in cable screen during work with one-sided ungrounded cable screen. *Energies*, 14, 4263. https://doi.org/10.3390/en14144263
- Scott-Meyer, W. (1982). *EMTP Rule Book Mode 31*. Portland, Oregon: B.P.A, USA.
- Sutton, S. J. (2017). High stress wet aging of cable dielectrics-meeting new challenges. *IEEE Electrical Insulation Magazine*, 33(1), 7-14. https://doi.org/10.1109/mei.2017.7804311
- Uribe, F. A. & Flores, J. (2018). Parameter estimation of arbitrary-shaped electrical cables through an image processing technique. *Electr. Eng.* 100, 1749-1759. https://doi.org/10.1007/s00202-017-0651-y
- Uribe, F., Ramos-Leaños, O., & Zuniga, P. (2023). An investigation of earth and sea-return impedances of power electrical cables. *Electric Power Systems Research*, 223, 109608. https://doi.org/10.1016/j.epsr.2023.109608
- Urquhart, A. J., & Thomson, M. (2015). Series impedance of distribution cables with sector-shaped conductors. *IET Generation Transmission & Distribution*, 9(16), 2679-2685. https://doi.org/10.1049/iet-gtd.2015.0546
- Wood, T., Finney, S., Macpherson, D., & Smith, C. (2012). HVDC networks for offshore wind power: current ripple and cables. Retrieved on https://doi.org/10.1049/cp.2012.2002

- Yin, Y. & Dommel, H. (1989). Calculation of frequency-dependent impedances of underground power cables with the finite element method. *IEEE Transactions on Magnetics*, 25(4), 3025-3027. https://doi.org/10.1109/20.34358
- Zhang, L., Tian, X., Boggs, S. A., & Bartolucci, E. J. (2011). Determination of total resistive loss in a multiple-circuit, Three-Phase cable system. *IEEE Transactions on Power Delivery*, 26(3), 1939-1945. https://doi.org/10.1109/tpwrd.2011.2142199

How to cite:

Elizalde-Camino, F., Padilla-González, M., Ruíz-Prieto, J. de J., Morales-Beltrán, J. R., Diaz-Santana, I., Hernández-Véliz, G., Ibarra-Torres, J. C., & Uribe-Campos, F. A. (2025). A conductor subdivision-based method for underground power cable impedance estimation. *Ingeniería Investigación y Tecnología*, 26(04),1-13.https://doi.org/10.22201/fi.25940732e.2025.26.4.032